ELSEVIER

Bone 39 (2006) 616–622

BONE

www.elsevier.com/locate/bone

Pamidronate does not adversely affect bone intrinsic material properties in children with osteogenesis imperfecta

Markus Weber [a,c], Paul Roschger [a], Nadja Fratzl-Zelman [a,*], Thomas Schöberl [c], Frank Rauch [b], Francis H. Glorieux [b], Peter Fratzl [d], Klaus Klaushofer [a]

[a] *Ludwig Boltzmann Institute of Osteology at the Hanusch Hospital of WGKK and AUVA Trauma Centre Meidling, 4th Med. Dept., Hanusch Hospital, Heinrich Collin Str. 30, A-1140 Vienna, Austria*

[b] *Genetics Unit, Shriners Hospital for Children and McGill University, Montreal, Quebec, Canada QCH3 G1A6*

[c] *Erich Schmid Institute of Materials Science, Austrian Academy of Sciences and Institute of Metal Physics, University of Leoben, A-8700 Leoben, Austria*

[d] *Max Planck Institute of Colloids and Interfaces, Dept. Biomaterials, D-14424 Potsdam, Germany*

Received 16 August 2005; revised 21 February 2006; accepted 24 February 2006
Available online 17 April 2006

Abstract

Cyclical intravenous pamidronate therapy increases bone mass in children with osteogenesis imperfecta (OI), but the effect on the intrinsic material properties of bone is unknown at present. Thus, a possible influence of pamidronate treatment on bone quality at the material level might negate the beneficial effects of the gain in bone mass and lead to bone fragility in the long term. In the present study, we used transiliac bone biopsy samples and assessed the intrinsic material properties of the bone tissue at the micron-level by combined backscattered electron imaging and nanoindentation.

Paired iliac bone samples from 14 patients (age 3 to 17 years) with severe OI before and after 2.5 ± 0.5 years (mean ± SD) of pamidronate treatment as well as age-matched controls were examined. Bone histomorphometry was performed in all samples and confirmed an increase of bone mass in treated patients. Backscattered electron imaging was used to measure the weighted mean calcium content (Ca_{Mean}), the most frequent calcium content (Ca_{Peak}), the variation in mineralization (Ca_{Width}) and the amount of lowly mineralized areas (Ca_{Low}) that correspond to sites of primary mineralization. Nanoindentation was performed in a subgroup of 6 patients and 6 controls to determine hardness and elastic modulus.

Compared to controls, untreated OI patients had a significantly higher degree of bone matrix mineralization (Ca_{Peak} +7%, $P < 0.001$) and a strong reduction of Ca_{Low} (−38%, $P < 0.001$) despite enhanced bone formation, as well as increased hardness (+21%, $P < 0.01$) and elastic modulus (+13%, $P < 0.01$). However, none of these parameters was significantly altered by the subsequent pamidronate treatment. This shows that OI bone is stiffer and more mineralized and that, despite the enhanced bone formation rate in these patients, areas of primary mineralization are hardly visible.

We also conclude that pamidronate treatment in children with OI does not have an adverse effect on the intrinsic material properties of bone and, as a consequence, that a long-term administration of the drug might not increase brittleness and fragility of the bone matrix. The antifracture effectiveness of pamidronate treatment in OI, as shown in previous clinical studies, has to be explained by the increase of mainly cortical bone volume.

Keywords: Osteogenesis imperfecta; Children; Pamidronate; Intrinsic bone material properties; Nanoindentation; Quantitative backscattered electron imaging

Introduction

Osteogenesis imperfecta (OI) is a heterogeneous heritable disorder that is characterized by low bone mass and increased bone fragility [1]. In most patients, the disease is caused by mutations in one of the two genes that code for collagen type I alpha chains (COL1A1 and COL1A2) [1]. Whereas the genetic

* Corresponding author. Ludwig Boltzmann Institute of Osteology, UKH Meidling, Kundratstrasse 37, A-1120 Vienna, Austria. Fax: +43 1 60150 2651.
E-mail address: nadja.fratzl-zelman@osteologie.at (N. Fratzl-Zelman).

8756-3282/$ - see front matter © 2006 Elsevier Inc. All rights reserved.
doi:10.1016/j.bone.2006.02.071

background of OI and the resulting defects in collagen structure have become increasingly well characterized, there is still little understanding of the mechanisms leading to the marked bone fragility in OI [2]. In particular, it is not clear to what extent the increased susceptibility to bone fractures results from diminished bone mass or rather is the consequence of impaired bone material quality.

Iliac bone samples of children with OI are abnormally small, have thin cortices and a low amount of trabecular bone [3]. The activity of both bone formation and bone resorption is increased and the lamellar organization of trabeculae appears disordered, reflecting a disturbed bone matrix architecture [1]. One study has found that children with OI have hypermineralized bone matrix [4]. Similar observations have been made in the *oim*, a murine model of moderate-to-severe OI. The bones of these animals exhibit an abnormally high calcium concentration but a low amount and poorly cross-linked collagen fibrils [5], leading to increased hardness of the matrix combined with reduced mechanical strength [6–8].

In the past few years, therapy with intravenous pamidronate has been reported to increase bone mass and to decrease fracture rates in children with severe OI [1]. Histomorphometric studies suggest that the increase in bone mass is due to higher cortical thickness and a larger number of trabeculae [9]. While the improvement in fracture incidence probably can be explained by the increase in bone mass, it is not known to what extent the treatment also affects the intrinsic material properties of the bone matrix.

Intrinsic material properties of bone tissue are defined by the composition of the organic matrix and its degree of mineralization at the ultrastructural level and are independent of bone mass, geometry and trabecular structures. At the present time, little is known about the quality of bone formed in the course of pamidronate therapy. However, this question is of crucial importance since bisphosphonates are known to increase the degree and homogeneity of mineralization in patients with postmenopausal osteoporosis [10,11]. The bone matrix of OI patients is known to be already hypermineralized prior to therapy [1]. Therefore, there are concerns that bisphosphonate treatment might further increase the brittleness and therefore fragility of OI bone [12].

In a previous study, we have shown that alendronate treatment does not alter the mechanical and material properties of bone in the *oim* mouse model, a rather encouraging perspective for the bisphosphonate therapy in children with OI [13]. But until now, there is no evidence that the same is true in treated children. One difficulty is that biomechanical properties of bone cannot be studied in humans by conventional methods like whole-bone bending tests. To determine bone stiffness and hardness within bone biopsies, we used nanoindentation, a well-established technique to assess the intrinsic mechanical properties of human bone and cartilage [14–16].

In the present study, we compare bone histomorphometric data, the degree of mineralization of the bone matrix and the mechanical properties of bone material in 14 children with OI. Paired iliac bone samples were taken and evaluated before and after a 2.5-year pamidronate therapy as well as in age-matched controls.

Materials and methods

Subjects

The study population comprised 14 patients (6 girls, 8 boys) with moderate to severe OI that were treated at the Shriners Hospital for Children in Montreal. These subjects are a subgroup of the cohort whose histomorphometric results during pamidronate treatment have been reported earlier [9]. The distribution of OI types was as follows: Type I, $N = 4$; type III, $N = 3$; type IV, $N = 7$. Collagen type I mutations were assessed as described previously [17]. Mutations were found in 12 of these patients, in one patient no collagen type I mutation was detectable by sequence analysis, and one patient had not been tested.

The indications for pamidronate treatment were one or more of the following situations: long-bone deformities; more than two fractures per year during the previous 2 years; vertebral compression fractures. Age at the time of the pretreatment biopsy ranged from 3.6 to 17.5 years. At the time of the second biopsy, these patients had received pamidronate therapy for 2.5 ± 0.5 years (mean ± SD; range 1.2 to 3.4 years). Pamidronate was administered intravenously on three consecutive days at a dose of 1 mg/kg daily in all patients, as described [1]. Such 3-day cycles were repeated every 4 months, resulting in a total annual dose of 9 mg per kg body weight. Results in the study group were compared to those from 14 age-matched children (8 girls, 6 boys; age 3.6 to 17.0 years) who were free from metabolic bone disorders, as described earlier [18]. These children had undergone iliac bone biopsies during unrelated orthopedic procedures. These biopsy samples had been obtained with the aim of establishing reference data for pediatric histomorphometry [18]. The study was approved by the Shriners Hospital Institutional Review Board, and informed consent was obtained from the legal guardians.

Nanoindentation was performed in a subset of 6 OI patients (3 girls, 3 boys; age at the time of the first biopsy 10.0 to 15.3 years) and 6 controls (3 girls, 3 boys; age 9.1 to 14.6 years). One of the OI patients was diagnosed with OI type III, the other 5 were classified as having OI type IV. The biopsy in control patients was obtained during corrective surgery for talipes equinovarus.

Bone densitometry

Bone densitometry was performed by dual-energy X-ray absorptiometry in the antero-posterior direction at the lumbar spine (L1–L4) using a Hologic QDR 2000W or 4500A device (Hologic Inc., Waltham, MA). Volumetric bone mineral density was derived as described by Carter et al. [19] using the formula:

$$\text{volumetric bone mineral density} = (\text{bone mineral content})/(\text{projection area})^{1.5}$$

Bone biopsy and histomorphometry

Whenever possible, labeling was performed prior to biopsy using demeclocycline (15–20 mg/kg per day taken orally during two 2-day periods separated by a 10-day free interval). This labeling course was completed before the biopsy procedure in all study participants except for two of the control subjects. Transiliac bone samples were collected 4 or 5 days after the labeling. Samples were processed undecalcified and were embedded in polymethylmethacrylate as described previously [18]. Measurements were carried out using a digitizing table with Osteomeasure® software (Osteometrics Inc., Atlanta, GA). Nomenclature and abbreviations follow the recommendations of the American Society for Bone and Mineral Research [20].

Quantitative backscattered electron imaging (qBEI)

The bone mineralization density distribution (BMDD) was determined in trabecular bone by qBEI. Full details of the technique and its precision have been published previously [21,22]. Blocks containing polymethylmethacrylate-embedded undecalcified iliac bone samples were prepared for qBEI by grinding

and polishing in order to obtain planoparallel surfaces. Subsequently, the sample surface was carbon coated prior to qBEI in the scanning electron microscope. A digital scanning electron microscope (DSM 962, Zeiss, Oberkochen, Germany) equipped with a four-quadrant semiconductor backscattered electron detector was employed. The accelerating voltage of the electron beam was adjusted to 20 kV, the probe current to 110 pA and the working distance to 15 mm. The entire trabecular bone tissue area was recorded by images of the same size (1 mm × 1.25 mm) at 100× nominal magnification, corresponding to a resolution of 2 μm per pixel. A scan speed of 100 s per frame was used. The qBEI images were converted into gray level histograms that displayed the percentage of mineralized bone area occupied by a certain gray level. These gray levels were transformed to weight percent Ca values by the following method: first, the gray scale was calibrated using the atomic number contrast between carbon (Z = 6) and aluminum (Z = 13) as reference materials. The brightness and contrast control of the BE detector were adjusted prior to each imaging run so that the gray level index of carbon was set to 25 and that of aluminum to 225. Second, the calibrated gray scale was converted into weight percent Ca by measuring once the gray value of osteoid (unmineralized collagen, corresponding to 0 wt.% Ca) and pure hydroxyapatite (corresponding to 39.86 wt.% Ca) as references. Gray levels were then transformed into weight percent Ca by a linear interpolation between the osteoid and hydroxyapatite gray level. A histogram bin width of 0.17 wt.% Ca was thus achieved.

Four parameters were deduced from the BMDD: Ca_{Mean}, the weighted mean Ca-concentration of the bone area; Ca_{Peak}, the peak position of the histogram, which indicates the typical calcium concentration in the sample; Ca_{Width}, the full width at half maximum of the distribution, describing the variation in mineralization density; and Ca_{Low}, the amount of bone area which is mineralized at less than 17.68 wt.% Ca. This specific Ca cutoff value was derived from the BMDD of normal adults and divides the entire range of mineralization in a range of higher and lower mineralization density covering 95% and 5% of the bone area, respectively [22]. Additionally, it was found that areas undergoing primary mineralization as marked by tetracycline fluorescence labeling have a mineral content at about 18 wt.% Ca, which is comparable to that of the Ca cutoff value above [23]. Therefore we interpret Ca_{Low} to reflect the percentage of primary mineralized bone.

Nanoindentation

Quasi-static nanoindentation tests were performed on the same bone sections used for qBEI measurements. A combination of an atomic force microscope (Digital Instruments, Veeco Metrology Group, Woodbury, NY) and an add-on nanoindentation device (Hysitron Inc., Minneapolis, MN) was used. The nanoindentation device consists of a three-plate capacitor. When a voltage is applied on the outer plates, the electrostatic force on the center plate drives the indenter into the sample (Fig. 1). The changes in electrostatic capacity due to the center plate displacement serves as a measure for the penetration of the indenter into the sample. The instrumental resolution is 100 nN for the force and 0.2 nm for the displacement. A Berkovich three-sided pyramidal tip was used as indentor. The indents were performed in a quasi load-controlled manner (i.e. there was no feed-back control for the loading force).

The combination of an atomic force microscope with an add-on nanoindentation device allows for imaging the surface topography and performing indentations with the same tip, so that the location of the indent can be chosen with high accuracy. Moreover, an image of the indented surface can be taken immediately after the indentation (Fig. 1).

A complete loading–unloading cycle consisted of five linear segments (Fig. 1). A linear loading phase of 5 s (segment 1) is followed by a 60 s holding period at a maximum force of 5 mN (segment 2). This leads to indentation depths of 500–700 nm, depending on the stiffness and hardness of the tested region. Unloading was performed in three steps: a linear unloading segment of 10 s down to 1 mN (segment 3), a holding period of 20 s (segment 4) and a further linear unloading down to zero load (segment 5). The holding time at maximum load was comparable to that found usually in the literature for nanoindentation in bone [24]. This length of holding time ensures that the largest portion of creep was finished before the start of unloading (segment 3). A large amount of creep during unloading would have a noticeable influence on the slope of the unloading curve, resulting in an overestimation of stiffness. The second holding

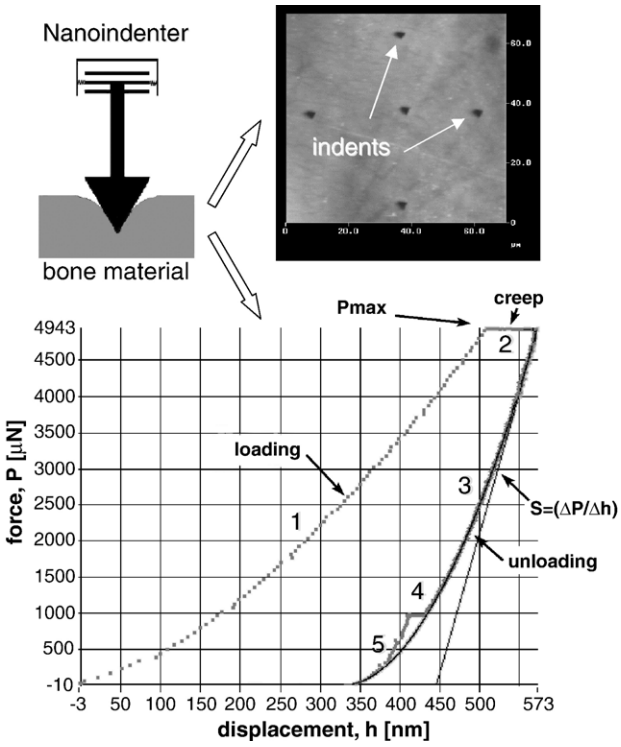

Fig. 1. Scheme of the nanoindentation measurements: Force (P) displacement (h) diagram composed by 5 segments: (1) linear loading, (2) holding, (3) initial unloading, (4) holding, (5) final unloading. Slope (S) indicates the E-modulus. Image above shows indents in bone surface immediately after indentation using the indenter tip also for imaging.

time at 20% of the maximum load (segment 4) served mainly as a control of the thermal drift of the instrument.

Elastic modulus and hardness were extracted from the first unloading curve, using the Oliver–Pharr-method [25]. In this study, the elastic modulus was measured as the so-called reduced modulus. Thus, the elasticity of the diamond tip is considered negligible, which is justified by the fact that the elastic stiffness of diamond is about 50 times that of bone.

Nanoindentation was performed in both the cortical and the trabecular region of the biopsies. No statistically significant difference was found between indents in either region, so all the measurements were analyzed together, especially as very small amount of materials was available in general from the OI patients. Areas suitable for analysis were identified by reflected light microscopy. Five indents were performed in each of the 9 to 15 selected indentation regions per sample. One of the five indents per region was placed in the center of a rectangle. The other four indents were placed at a distance of 25 μm from the central indent at the corners of the rectangle (Fig. 1). After indentation, imaging was performed in order to identify potential artifacts, such as indents that had erroneously been placed in embedding material inside haversian canals or very close to edges of bone material. This method of grouped indentations covers areas of about 50 μm × 50 μm each, on the sample surface and targets preferentially mature bone matrix, because mature bone exhibits the major part of the bone area (96%) compared to less than 4% of newly formed bone (see Ca_{Low} values in Table 1). In addition, the new bone is located preferentially on the bone surface, sites generally excluded from indentation. Hardness and E-modulus were calculated as the mean values for each subject.

Statistics

Differences between results at baseline and during Pamidronate treatment were tested for significance using paired t tests. Comparisons between controls and results in OI patients at the two time points were performed by one-way analysis of variance (ANOVA), followed by Fisher's PLSD post hoc test. $P < 0.05$ was considered statistically significant. Statistical analyses were

Table 1
Results in controls and the OI study population before and during pamidronate treatment

	Control	OI before pamidronate	OI during pamidronate	P^a	P^b
Age (years)	9.4 (3.8)	9.3 (4.0)	11.9 (3.9)	0.96	–
Histomorphometry					
Core width (mm)	7.2 (1.9)	3.4 (1.2)	3.8 (1.7)	<0.001	0.48
Cortical width (μm)	822 (199)	447 (202)	639 (228)	<0.001	0.005
Bone volume per tissue volume (%)	21.7 (4.7)	9.6 (4.7)	11.3 (6.1)	<0.001	0.25
Trabecular thickness (μm)	125 (21)	108 (238)	105 (23)	0.05	0.69
Trabecular number (/mm)	1.74 (0.26)	0.88 (0.30)	1.04 (0.48)	<0.001	0.17
Mineral apposition rate (μm/day)	0.94 (0.09)	0.67 (0.18)	0.60 (0.16)	<0.001	0.20
Bone formation rate per bone surface ($\mu m^3\ \mu m^{-2}\ year^{-1}$)	44 (21)	66 (26)	20 (22)	0.03	<0.001
qBEI					
Ca_{Mean} (%)	20.96 (0.56)	22.62 (0.66)	22.54 (0.64)	<0.001	0.74
Ca_{Peak} (%)	21.65 (0.59)	23.22 (0.58)	23.05 (0.68)	<0.001	0.51
Ca_{Width} (%)	3.48 (0.35)	3.50 (0.33)	3.38 (0.39)	0.85	0.34
Ca_{Low} (%)	6.85 (1.65)	4.25 (1.45)	3.64 (1.50)	<0.001	0.27
Nanoindentation					
Hardness (GPa)	0.67 (0.05)	0.81 (0.08)	0.83 (0.11)	0.01	0.69
E-modulus (GPa)	18.8 (1.1)	21.3 (1.5)	22.1 (2.0)	0.01	0.43

Values represent mean (SD).
[a] Independent *t* test between control and OI before pamidronate treatment.
[b] Dependent *t* test between OI time points.

performed using StatView 4.0 software (Abacus concepts, Inc., Berkeley, CA, USA).

Results

The histomorphometric and densitometric results showed the expected increase in bone mass and cortical thickness in OI patients during pamidronate treatment, as previously described [9]. Pretreatment iliac bone samples of OI patients were smaller than those of control patients (Table 1, Fig. 2A), had thinner cortices and less trabecular bone (Table 1, Fig. 2B), but higher trabecular bone formation rates. Cortical width increased during pamidronate treatment (Table 1, Fig. 2C). Cancellous bone volume also increased numerically, but this was not statistically significant (Table 1). Lumbar spine densitometry in OI patients revealed a rise in lumbar spine bone mineral content from 10.1 g (SD 7.5 g) to 20.0 g (9.9 g) and in volumetric bone mineral density from 71 mg/cm^3 (26 mg/cm^3) to 96 mg/cm^3 (20 mg/cm^3) during the study interval ($P < 0.001$ in both cases).

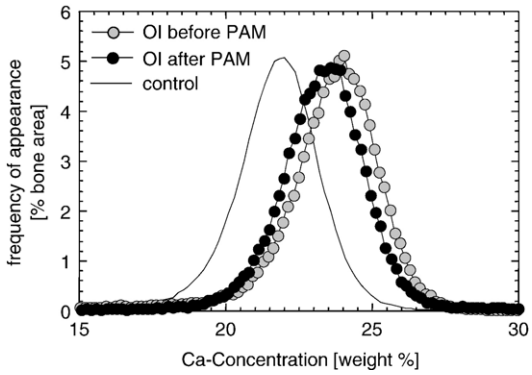

Fig. 3. Representative examples of BMDDs. Data correspond to the results of the samples shown in Fig. 2.

The qBEI evaluations showed that the typical calcium content (Ca_{Peak}) was significantly increased (+7%, $P < 0.001$) in OI patients independently of pamidronate treatment. Statistical analysis by paired *t* test as well by one-way ANOVA did not reveal any changes of Ca_{Peak} in OI bone before and after treatment (Table 1, Fig. 3). Interestingly, the higher degree of matrix mineralization was accompanied in all OI patients by a strong reduction of low mineralized bone areas (Ca_{Low}). Indeed, bone matrix areas with a low calcium content (17.68 wt.% or less) corresponding to areas of primary mineralization were markedly less frequent (−38%) in OI than in controls. Again, analysis by paired *t* test as well by one-way ANOVA did not reveal any changes of Ca_{Low} in OI after pamidronate treatment (Table 1). The uniformity of mineralization (Ca_{Width}) was similar in all three groups (Table 1).

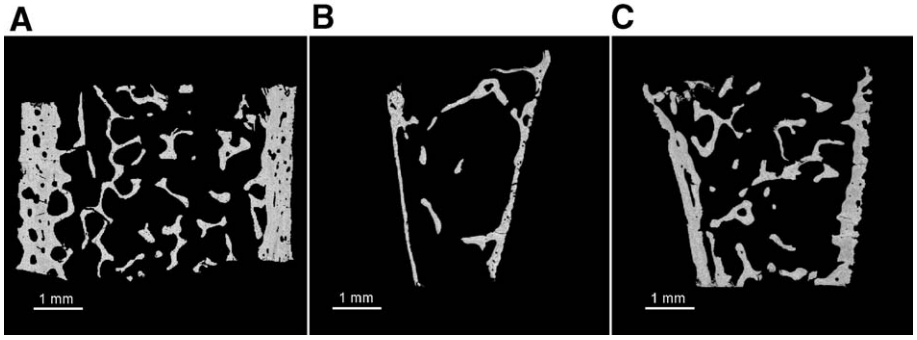

Fig. 2. qBEI images of transiliac bone samples. (A) Control sample age matched. (B) Pretreatment sample from a 6 year-old girl with OI type III caused by a mutation in the COL1A1 gene. (C) Specimen from the same patient after 2.8 years of pamidronate treatment.

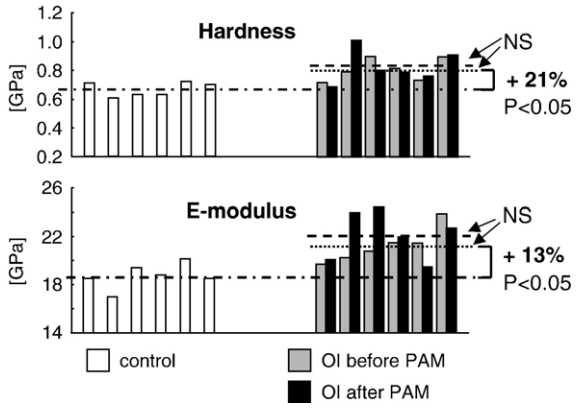

Fig. 4. Individual results for hardness and elastic modulus. The dashed-dotted line in each graph represents the mean of the control group. The dotted line in the OI bars represents the mean before and the dashed line after pamidronate (PAM) treatment.

Nanoindentation was performed in a subset of 6 OI patients and 6 controls. qBEI results in these individuals were similar to the data shown above. Hardness and the elastic indentation modulus were increased by +21% ($P < 0.01$) and by +13% ($P < 0.1$), respectively, in untreated OI patients compared to control samples. Again, these results were not altered by bisphosphonate therapy (Table 1, Fig. 4).

Discussion

The present study focused on the intrinsic bone material quality in children affected with severe osteogenesis imperfecta (OI types III and IV) and treated with the bisphosphonate pamidronate. Summarizing the results obtained in the present study, the following picture emerges: in agreement with previous studies on OI patients and on the OI murine (*oim*) model [1,6,7], the bone matrix appears to be more highly mineralized, leading to a higher stiffness and hardness of the bone material as measured for the first time in the present study by nanoindentation. The main finding regarding the bone mineral distribution is a shift towards generally higher mineral content for OI patients (that is, an increase in Ca_{peak}), with an extreme reduction of newly formed bone areas with low calcium content (Ca_{Low}). The last aspect is particularly surprising, as OI is associated with elevated bone turnover [1] and, therefore, one would expect to find a high proportion of matrix undergoing primary mineralization. The fact that this was not the case suggests that the abnormality in OI bone matrix is responsible for this effect. Possibly, the altered collagen structure in OI allows abnormally fast mineralization leading to the disappearance of lowly mineralized areas. However, none of the measured material properties was altered by pamidronate treatment.

Nanoindentation was applied to bone biopsies after fixation and embedding, a procedure, which might – in principle – lead to a modification of the mechanical properties of the bone matrix. However, all specimens – before and after treatment as well as the controls – were fixed in exactly the same way, so that we believe a comparison is possible despite the fixation. In addition, the results for human OI are in agreement with our previous study on the *oim* model [13], where it was shown by 3-point bending tests, that material properties like bone strength, stiffness, toughness, young modulus and moment of inertia were not affected by alendronate treatment. In contrast, in the wild-type mice, material and mechanical properties of bone were improved and bone mineralization increased due to the antiresorptive activity [13].

Our current results confirm that the only significant effect of pamidronate found in the present study for OI in humans is an increase in bone mass, mainly in the cortex, which is in agreement with results of previous studies of iliac bone biopsies [1,9] as well as lumbar spine [26] of affected patients. The reduced fracture incidence after pamidronate treatment is therefore most likely related to the increased amount of bone material, while the intrinsic material properties of bone tissue i.e., mineralization density or amount of mineral per volume of bone, as well as, stiffness and hardness remained unaffected.

Interestingly, this increase of cortical bone material is accompanied by a decreased bone turnover and does not really affect trabecular architecture. This is linked to the special situation in growing children where cortical bone is subjected to modeling (as bone is growing), while cancellous bone is remodeled. Indeed, osteoclasts remove bone on the inner surface of the cortex, while osteoblasts add bone on the outer cortex. Inhibiting the osteoclasts reduces turnover in cancellous bone and avoids thinning of the cortex from inside. The activity of osteoblasts on the outer side of the cortex is, however, not reduced. As a consequence, the cortex is thickening. In contrast, the cancellous space is mostly unaffected because the inhibition of osteoclast activity by the bisphosphonate leads to a corresponding decrease in osteoblast activity and thus, to a reduced remodeling rate. Consequently, trabecular thickness and architecture are not changing [1].

These results raise interesting questions about the origin of bone fragility in OI patients and the differential effects of bisphosphonates. It is clearly primarily the genetic defect in OI, leading to impaired collagen biosynthesis [1], which affects the quality of the bone material [5]. But the abnormally high material stiffness of OI bone may also play a role in the development of low bone mass in children with OI. It is widely assumed that osteocytes sense mechanical deformation inside the bone matrix [27]. Their signals are then used to initiate bone resorption and/or formation, depending on the mechanical needs. When the material stiffness is abnormally increased, as it is in children with OI, a given force will induce less bone matrix deformation than in healthy children. Osteocytes will therefore "underestimate" the real mechanical loads that are acting on the bone. The consequence is that bone mass and strength adaptation will lag behind the mechanical needs, thus creating a situation of osteopenia. A similar scenario has been put forward by Frost, who proposed that the clinical manifestations of OI can be explained by a disturbance of the mechanostat setpoint [28]. An alternative explanation is also possible using the model by Burr and coworkers [29] who assume that the stimulus for bone remodeling is microdamage rather than deformation. In this spirit, one could speculate that bone

fragility in OI patients leads to rapid accumulation of microdamage and, as a consequence, to enhanced remodeling activity. However, since the new bone matrix is not better in terms of mechanical competence, new signals will trigger even more osteoclastic activity. Thus, bone hypermineralization may be indirectly responsible for the increased remodeling activity in OI bone, which was also observed in the present samples.

A second interesting aspect of this study is that the bisphosphonate therapy induces no changes in the mineralization profile of OI, while according to the literature, bisphosphonate therapy results in an increase of mineralization of bone in postmenopausal osteoporosis [10,11]. However, this increase of mineral density was reported in patients with normal or lowered mineral density, like in osteoporosis, where the bone matrix is typically undermineralized [11,30]. In contrast, in human OI [4] as well as in the *oim* model [5–8,13], the bone matrix is already hypermineralized prior to treatment. Hence, a further increase upon treatment is not possible because of the inherent saturation of the matrix.

In conclusion, this study shows that OI bone is abnormally dense and stiff at the material level and that these intrinsic bone material properties are not affected by pamidronate treatment. The reduced fracture incidence after pamidronate treatment is solely due to the observed increase of cortical bone mass in combination with the growth of the patients. The results suggest that pamidronate therapy in children with OI is neither improving nor further deteriorating the already fragile bone material. The increased bone mass, however, represents a clear benefit for these patients.

Acknowledgments

We thank Rose Travers for histomorphometric analyses at the Genetics Unit of Shriners Hospital for Children, Montreal, and Gerda Dinst, Phaedra Messmer, Sonja Lueger for careful sample preparations and qBEI measurements at the bone material laboratory of the Ludwig Boltzmann-Institute of Osteology, Vienna, Austria. This study was supported by the Shriners of North America, by the AUVA (Austrian Social Insurance for Occupational Risk), by the WGKK (Social Health Insurance Vienna) and the FWF (The Austrian Science Fund) Project # P16880-B13.

References

[1] Rauch F, Glorieux FH. Osteogenesis imperfecta. Lancet 2004;363:1377–85.
[2] Fratzl P, Gupta HS, Paschalis EP, Roschger P. Structure and mechanical quality of the collagen–mineral nano-composite in bone. J Mater Chem 2004;14:2115–23.
[3] Rauch F, Travers R, Parfitt AM, Glorieux FH. Static and dynamic bone histomorphometry in children with osteogenesis imperfecta. Bone 2000;26:581–9.
[4] Boyde A, Travers R, Glorieux FH, Jones SJ. The mineralization density of iliac crest bone from children with osteogenesis imperfecta. Calcif Tissue Int 1999;64:185–90.
[5] Miles CA, Sims TJ, Camacho NP, Bailey AJ. The role of the alpha2 chain in the stabilization of the collagen type I heterotrimer: a study of the type I homotrimer in oim mouse tissues. J Mol Biol 2002;30:797–805.
[6] Fratzl P, Paris O, Klaushofer K, Landis WJ. Bone mineralization in an osteogenesis imperfecta mouse model studied by small-angle X-ray scattering. J Clin Invest 1996;97:396–402.
[7] Misof K, Landis WJ, Klaushofer K, Fratzl P. Collagen from the osteogenesis imperfecta mouse model (oim) shows reduced resistance against tensile stress. J Clin Invest 1997;100:40–5.
[8] Grabner B, Landis WJ, Roschger P, Rinnerthaler S, Peterlik H, Klaushofer K, et al. Age- and genotype-dependence of bone material properties in the osteogenesis imperfecta murine model (oim). Bone 2001;29:453–7.
[9] Rauch F, Travers R, Plotkin H, Glorieux FH. The effects of intravenous pamidronate on the bone tissue of children and adolescents with osteogenesis imperfecta. J Clin Invest 2002;110:1293–9.
[10] Boivin GY, Chavassieux PM, Santora AC, Yates J, Meunier PJ. Alendronate increases bone strength by increasing the mean degree of mineralization of bone tissue in osteoporotic women. Bone 2000;27:687–94.
[11] Roschger P, Rinnerthaler S, Yates J, Rodan GA, Fratzl P, Klaushofer K. Alendronate increases degree and uniformity of mineralization in cancellous bone and decreases the porosity in cortical bone of osteoporotic women. Bone 2001;29:185–91.
[12] Marini JC. Do bisphosphonates make children's bones better or brittle? N Engl J Med 2003;349:423–6.
[13] Misof BM, Roschger P, Baldini T, Raggio CL, Zraick V, Root L, et al. Differential effects of alendronate treatment on bone from growing osteogenesis imperfecta and wild-type mouse. Bone 2005;36:150–8.
[14] Rho JY, Tsui TY, Pharr GM. Elastic properties of human cortical and trabecular lamellar bone measured by nanoindentation. Biomaterials 1997;18:1325–30.
[15] Hengsberger S, Kulik A, Zysset P. A combined atomic force microscopy and nanoindentation technique to investigate the elastic properties of bone structural units. Eur Cell Mater 2001;1:12–7.
[16] Gupta HS, Schratter S, Tesch W, Roschger P, Berzlanovich A, Schoeberl T, et al. Two different correlations between nanoindentation modulus and mineral content in the bone–cartilage interface. J Struct Biol 2005;149:138–48.
[17] Korkko J, Ala-Kokko L, De Paepe A, Nuytinck L, Earley J, Prockop DJ. Analysis of the COL1A1 and COL1A2 genes by PCR amplification and scanning by conformation-sensitive gel electrophoresis identifies only COL1A1 mutations in 15 patients with osteogenesis imperfecta type I: identification of common sequences of null-allele mutations. Am J Hum Genet 1998;62:98–110.
[18] Glorieux FH, Travers R, Taylor A, Bowen JR, Rauch F, Norman M, et al. Normative data for iliac bone histomorphometry in growing children. Bone 2000;26:103–9.
[19] Carter DR, Bouxsein ML, Marcus R. New approaches for interpreting projected bone densitometry data. J Bone Miner Res 1992;7:137–45.
[20] Parfitt AM, Drezner MK, Glorieux FH, Kanis JA, Malluche H, Meunier PJ, et al. Bone histomorphometry: standardization of nomenclature, symbols, and units. Report of the ASBMR Histomorphometry Nomenclature Committee. J Bone Miner Res 1987;2:595–610.
[21] Roschger P, Fratzl P, Eschberger J, Klaushofer K. Validation of quantitative backscattered electron imaging for the measurement of mineral density distribution in human bone biopsies. Bone 1998;23:319–26.
[22] Roschger P, Gupta HS, Berzlanovich A, Ittner G, Dempster DW, Fratzl P, et al. Constant mineralization density distribution in cancellous human bone. Bone 2003;32:316–23.
[23] Misof BM, Roschger P, Cosman F, Kurland ES, Tesch W, Messmer P, et al. Effects of intermittent parathyroid hormone administration on bone mineralization density in iliac crest biopsies from patients with osteoporosis: a paired study before and after treatment. J Clin Endocrinol Metab 2003;88:1150–6.
[24] Zysset PK, Guo XE, Hoffler CE, Moore KE, Goldstein SA. Elastic modulus and hardness of cortical and trabecular bone lamellae measured by nanoindentation in the human femur. J Biomech 1999;32:1005–12.
[25] Oliver WC, Pharr GM. An improved technique for determining hardness

and elastic modulus using load and displacement sensing indentation experiments. J Mater Res 1992;7:1564–83.
[26] Rauch F, Plotkin H, Zeitlin L, Glorieux FH. Bone mass, size and density in children and adolescent with osteogenesis imperfecta: effect of intravenous Pamidronate therapy. J Bone Miner Res 2003;18: 610–4.
[27] Burger EH, Klein-Nulend J. Mechanotransduction in bone-role of the lacuno-canalicular network. FASEB J 1999;13:S101–12 [Suppl:].
[28] Frost HM. Osteogenesis imperfecta. The set point proposal (a possible causative mechanism). Clin Orthop 1987;216:280–97.
[29] Burr DB, Forwood MR, Fyhrie DP, Martin RB, Schaffler MB, Turner CH. Bone microdamage and skeletal fragility in osteoporotic and stress fractures. J Bone Miner Res 1997;12:6–15.
[30] Stepan JJ, Alenfeld F, Boivin G, Feyen JH, Lakatos P. Mechanisms of action of antiresorptive therapies of postmenopausal osteoporosis. Endocr Regul 2003;37:225–38.